Catalysis Today 147 (2009) 217–223

Contents lists available at ScienceDirect

Catalysis Today

journal homepage: www.elsevier.com/locate/cattod

Characterization of Pt/SBA-15 prepared by the deposition–precipitation method

Svatopluk Chytil [1], Wilhelm R. Glomm, Edd A. Blekkan *

Department of Chemical Engineering, Norwegian University of Science and Technology (NTNU), NO-7491 Trondheim, Norway

ARTICLE INFO

Article history:
Available online 28 October 2008

Keywords:
Mesoporous silica
Deposition–precipitation
Pt
Silanols
Short-range order

ABSTRACT

Mesoporous silica SBA-15 was prepared and loaded with Pt using the deposition–precipitation method (DP). The Pt loaded material was characterized by N_2 sorption, and X-ray diffraction (XRD) at low scattering angles as well as XRD at wide angles, in order to monitor the impact of the metal deposition pathway on the mesoporous texture. After DP the material contains ordered mesoporous silica as well as a fraction appearing as non-ordered amorphous silica. This is most likely caused by the hydrothermal treatment involved in the DP. The material was also characterized using NIR and ^{29}Si MAS NMR spectroscopy. The NIR results of the calcined materials indicate that the silanol groups of SBA-15 may act as anchoring groups for the metallic Pt particles. The NMR spectroscopy data shows that the Pt/SBA-15 sample prepared by the DP method posseses a better short-range regularity of SBA-15 walls as compared to the parent SBA-15. This is suggested to be caused by dissolution and possible re-precipitation of siliceous species.

1. Introduction

SBA-15 is a mesoporous ordered silica with promising properties as a catalyst support [1,2]. A number of studies describing the use of the deposition–precipitation (DP) process for various systems can be found in the literature [3–11]. From these studies it can be concluded that nucleation and growth of the precipitated metal species is accompanied by a significant interaction between the support and the metal, underlining the complexity of the process. However, when metals are deposited on SBA-15 in this way, another variable must be considered; the relatively low hydrothermal stability of the mesoporous framework [12,13]. As there is a severe treatment involved in the DP method described here (heating the material at 90 °C in water for approximately 20 h), it is reasonable to expect changes in the textural properties of the SBA-15. Information concerning the interaction between the precipitated species and the support is usually obtained by monitoring the pH profile during the DP process [6,8,10]. This has been discussed in an earlier study, and a model for the interaction between the introduced Pt metal species and the SBA-15 support was suggested [14].

In this study we have attempted to elucidate some of these aspects by means of N_2 adsorption–desorption and X-ray diffraction (XRD) at low scattering angles. Furthermore, we present data obtained from wide-angle X-ray-diffraction and ^{29}Si MAS NMR spectroscopy recorded on the investigated solids in order to monitor the impact of the DP treatment on the parent SBA-15. We also demonstrate the use of NIR spectroscopy to further characterize the nature of Pt–SBA-15 interaction existing in the calcined solids.

2. Experimental

2.1. Sample preparation

The synthesis of the SBA-15 support was done following Stucky and co-workers [1] using a synthesis temperature of 100 °C. The material was calcined at 550 °C, and used as a support for Pt catalysts. Pt/SBA-15, DP was prepared by deposition–precipitation using an aqueous solution of $Pt(NH_3)_4(OH)_2$, while Pt/SBA-15, WI was prepared by aqueous wet impregnation of $H_2PtCl_6{\cdot}6H_2O$. Both catalysts were calcined at 300 °C. The details of the preparations are given elsewhere [14], and some characteristic data is summarized in Table 1. Blank experiments were also performed where the parent SBA-15 was exposed to the identical treatment involved in the functionalization pathways in the absence of the Pt precursors. Briefly, for the DP method the parent SBA-15 (3 g) was exposed to an aqueous solution containing urea (deionised water 250 ml, urea 0.026 g). The suspension was acidified by 0.1 M HNO_3,

* Corresponding author. Tel.: +47 73 59 41 57; fax: +47 73 59 40 80.
E-mail address: blekkan@nt.ntnu.no (E.A. Blekkan).
[1] Present address: SINTEF Materials and Chemistry, NO-7465 Trondheim, Norway.

0920-5861/$ – see front matter © 2008 Elsevier B.V. All rights reserved.
doi:10.1016/j.cattod.2008.09.003

heated to 90 °C and subsequently kept at this temperature for 20 h. Afterwards, the solids were recovered by filtration and washed by deionised water (200 ml). The washed material was dried in an oven at 80 °C for 17 h and finally calcined in flowing air at 300 °C for 2 h. This sample is assigned Pt/SBA-15, DP *treated*. The *SBA-15*, WI, *treated* sample was prepared by bringing SBA-15 into contact with an aqueous solution having a pH of 3 (adjusted using 2 M HCl). The sample was subsequently dried at 80 °C for 17 h, followed by calcination at 300 °C for 2 h.

2.2. Instrumentation

X-ray powder diffraction data was recorded on a Siemens D-5005 diffractometer using Cu Kα-radiation (λ = 1.542 Å). Nitrogen adsorption–desorption isotherms were measured using a Micromeritics TriStar 3000. Prior to the measurement, the samples were outgassed at 100 °C for 12 h. The specific surface area of the solids was evaluated by the BET method in the range of relative pressures p/p_0 = 0.1–0.3. The pore size distributions were obtained from desorption branch of the isotherm using the Broekhoff–De Boer algorithms. Micropore volumes were assessed by means of a *t*-plot analysis.

Diffuse-reflectance near infrared spectra were collected using a Bruker optics multi-purpose analyzer equipped with an integrating sphere attachment. In order to ascertain that none of the probe light was transmitted through the sample, spectra were taken with increasing sample amounts until no further increase in obtained spectra could be observed. The minimum sample size used for these analyses was then ~15% larger than the amount at which no further spectral changes could be observed. All NIR spectra were measured at ambient conditions. For clarity, NIR results are displayed as absorbance spectra. Identical spectra were recorded after a period of several weeks as well as from different batches of the same material, indicating very good reproducibility of the measurements. Upon the preparation of the samples, the solids were kept in sealed containers in order to avoid any contact with water/humidity. Thus the water present in the samples is most probably the remaining water from the preparation procedure.

The ^{29}Si MAS NMR spectra were collected using a Varian VXR S spectrometer with a 7.05T (tesla) wide-bore Oxford magnet, where the ^{29}Si frequency is 58.58 MHz. The MAS experiments were performed with a Jacobsen VT CP/MAS probe equipped with 7 mm ZrO_2 rotors at a spinning rate of 4.5 kHz. The ^{29} Si MAS experiments were run with a delay, d1, between the pulses of 5 s, a puls width of 6 μs, where pw90 is 8 μs and a number of scans of 20000 in each experiment. The ^{29}Si chemical shifts were referenced to tetramethylsilane. Instrumental neutron activation analysis (INAA) was used to measure the Pt loading in the samples. The solids were irradiated in the 2 MW JEEP II reactor, at Kjeller, Norway, together with standard materials of known elemental composition. After an appropriate decay period, high resolution spectrometry was used to measure the intensity and energies of the gamma lines emitted. A comparison between specific activities induced in standards and samples provides the basis for calculation of elemental abundances.

3. Results and discussion

3.1. Impact of the DP on textural and crystallographic properties of SBA-15

The impact of the preparation method was first studied by use of N_2 adsorption–desorption and X-ray diffraction at low diffraction angles. N_2 sorption isotherms and XRD patterns are depicted in Figs. 1 and 2 respectively, and stuctural parameters of the investigated solids are shown in Table 1. Clearly, the application of the DP leads to systematic changes of the parent SBA-15 such as an expansion of the mesopores and lowering of BET surface area. The surface area of the Pt/SBA-15, DP sample is reduced by approximately 70%. Furthermore, another important feature of the N_2 sorption isotherm is that the hysteresis loop is tilted, reflecting a less narrow pore size distribution [15]. These structural parameters as well as the shape of the hysteresis loop resemble those as obtained for SBA-15 prepared at higher temperatures (140–150 °C) [16]. Such materials are expected to possess a lower degree of mesoscopic order as at these synthesis temperatures the copolymer used as a structure directing agent tends to decompose. However, the shape of the hysteresis loop also resembles those obtained on amorphous non-ordered silicas as it is extended to high values of relative pressures p/p_0. This therefore implies that the functionalized material contains fractions of both; ordered mesoporous silica as well as non-ordered amorphous silica.

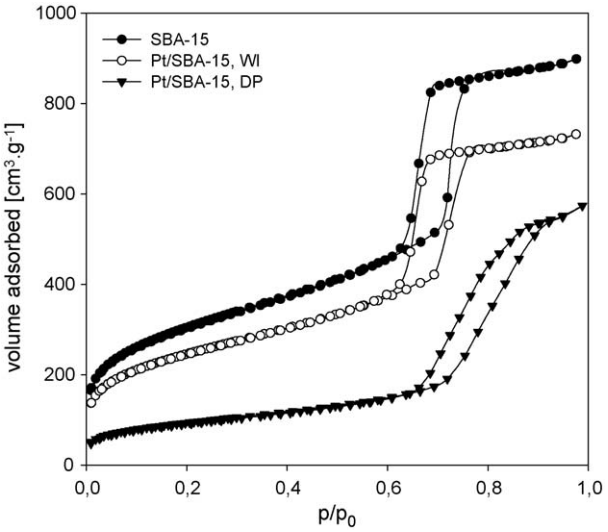

Fig. 1. N_2 sorption isotherms of SBA-15 and Pt/SBA materials.

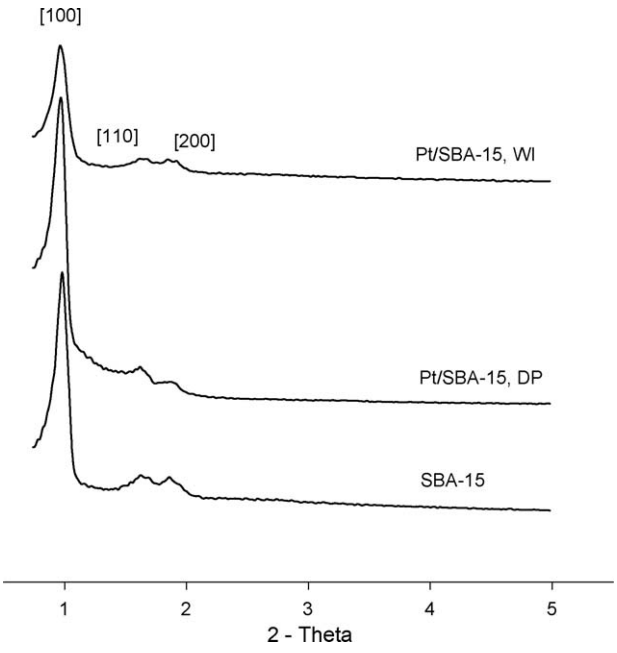

Fig. 2. Low angle XRD patterns of SBA-15 and Pt/SBA-15 materials.

The XRD data shows that the inclusion of Pt by the DP method does not interfere with the structural ordering of the mesoporous material, as there are no significant alterations of the diffraction lineshape of the functionalized materials compared to the parent SBA-15. A slight shift of the prominent XRD reflection [1 0 0] towards a lower angle is observed for the functionalized SBA-15, also similar to that detected for parent SBA-15 prepared at higher temperature or platinum supported on SBA-15 [16–18]. The apparent discrepancy between the conclusions derived from N_2 adsorption–desorption measurement is caused by the fact that the low angle XRD scattering measurement detects only the preserved hexagonally ordered SBA-15, while the N_2 sorption occurs on the ordered SBA-15 phase as well as on the non-ordered amorphous silica. Newertheless, the estimation of the proportional amount of the ordered and non-ordered silica presented in Pt/SBA-15, DP is rather difficult. It also follows that the value of wall thickness as derived from the combination of the XRD and N_2 sorption data has to be interpreted with some caution.

However, it is likely that the structural changes in SBA-15 upon the DP treatment towards the apparent disorder are caused by the treatment involved in the method.

The wide-angle XRD of Pt/SBA-15, WI (Fig. 3) shows reflections at $2\theta = 39.7^\circ$, 46.2° and 67.4°, attributed to the cubic platinum metal structure [20]. The most intense reflection (39.7°) was used to estimate the average platinum particle size to be 5.4 nm using the Scherrer formula. This is in good agreement with values obtained from TEM on the same material, where the majority of the Pt nanoparticles was found to be in the range 4–6 nm [14]. The Pt/SBA-15, DP sample did not exhibit similar intense reflections of metallic platinum, which is probably due to the lower metal loading (Table 1), i.e. the signal might have been below the sensitivity of the instrument, or that the particle size is below the detection threshold, typically estimated to be 3 nm. Here, the Pt particle size as observed by transmission electron microscopy (TEM) was found to be between 2 and 4 nm, however, a certain fraction of larger particles having a diameter of 15 nm was also detected [14]. No platinum oxide phase was detected in either case, see also [19] and references therein.

An interesting feature of the presented XRD patterns is the broad reflection centered at $2\theta = 23^\circ$ that was assigned to amorphous SiO_2 [21]. This reflection is considerably sharper for the Pt/SBA-15, DP sample, which might be related to changes in the ordering towards further consolidation of the silica framework. Here it should be reemphasised that X-ray diffraction probes the long-range order of examinated materials, and as such can be used as a valuable complement to NMR spectroscopy giving information about the local ordering [22,23].

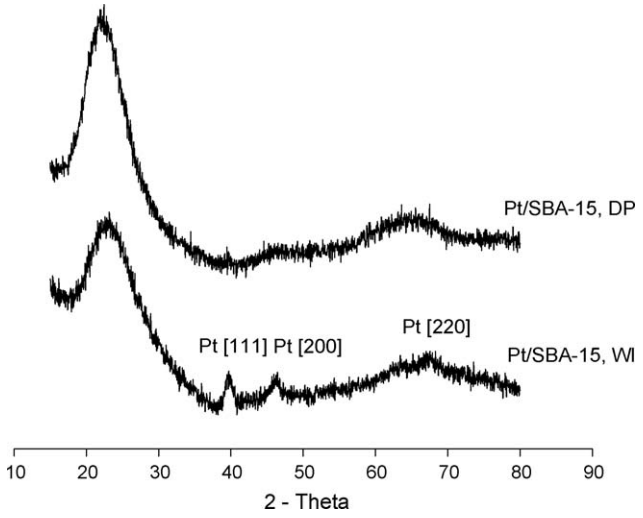

Fig. 3. Wide-angle X-ray diffraction patterns of Pt/SBA materials.

3.2. NIR characterization of SBA-15 and Pt/SBA-15

Silanol groups (believed to be the active species of SBA-15), their interaction with introduced platinum as well as the change in their population upon the heat treatment involved in preparation of Pt/SBA-15 samples have been studied with Diffuse-Reflectance near infrared (NIR) spectroscopy in the frequency region 8000–4000 cm^{-1} (overtone region, avoiding overlapping bands with adsorbed water). This method has been demonstrated to be useful for following silica surface modifications and is useful when the interaction between an active phase and the siliceous catalyst support is studied [24].

3.2.1. NIR of SBA-15

The diffuse-reflectance NIR spectrum of the calcined SBA-15 is shown in Fig. 4. The spectral region contains three sets of bands with prominent absorptions occurring at around 7300, 5270 and 4520 cm^{-1}. This is in a good agreement with NIR spectra recorded on other siliceous materials [25–28] including mesoporous silica MCM-41 [29]. In the first wavenumber region at 7300 cm^{-1}, a sharp peak situated at 7326 cm^{-1} is attributed to the first overtone of the stretching frequency of silanols (ν_{OH}) [25–27]. The bands at 7141 and 6856 cm^{-1} arise from isolated water molecules hydrogen bonded to silanol groups [26]. It has been shown that the strength of this donor hydrogen bond of silanols is similar to hydrogen bonds in γ-$Al(OH)_3$ [25]. Finally, a shoulder detected at 7425 cm^{-1} is ascribed to silanols which are perturbed by the interparticle contact [27,30].

Here it is important to emphasise that both vicinal free OH groups and isolated OH contribute to the prominent peak at 7326 cm^{-1}. On the other hand, geminal silanol groups, (two hydroxyl groups situated on one silicon atom), also occur on SBA-15, but cannot be monitored by NIR. The latter aspect will be discussed later in section dealing with ^{29}Si MAS NMR spectroscopy, as this method provides resolution between isolated and geminal silanol groups. Another aspect that should be considered in respect to the mesoporous silica SBA-15 is that the material contains silanols located in the inner surface of mesopores as well as on the outer surface. It has been shown that the large majority of silanol groups is located on the inner surface and the number of silanol groups has been estimated to be 3.7 SiOH/nm^2 [31]. Moreover, it

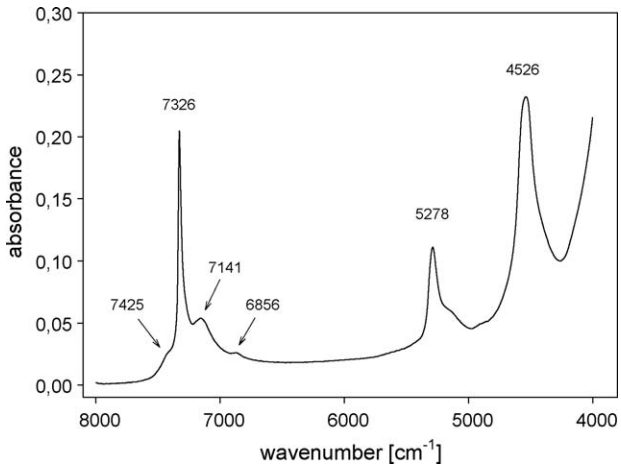

Fig. 4. Reflectance NIR spectrum of the first overtone region of SBA-15 calcined at 550 °C.

should be emphasised that in almost all kinds of amorphous silicas, there are silanols not only on the surface but also throughout the particle. These internal silanols arise in different ways depending on the process by which the silica is prepared. One source of internal SiOH groups is through diffusion of H_2O into the solid SiO_2 structure [32]. It has been pointed out that H_2O can penetrate into amorphous SiO_2 to a distance of 15 nm, where a small amount of silanols can exist as SiOH pairs [32]. Another source of internal silanols emanates from some of the SiOH located on the surface being trapped during the preparation procedure as the particles coalesce [33]. It should be noted that both internal and external SiOH groups contribute to the prominent silanol IR band at 3747 cm^{-1} [33] and therefore it is likely that they both also contribute to the overtone NIR silanol band at 7326 cm^{-1}.

The second region observed at around 5270 cm^{-1} is associated with the combination of stretching and deformation vibrations of water [26]. For a detailed description of the water interaction with SiOH groups see e.g. [25,26]. The asymmetrical broader band detected near 4520 cm^{-1} was assigned to a combination of the fundamental OH^- stretching of the isolated SiOH groups with the fundamental symmetric stretching mode of silica network at 800 cm^{-1} [27]. However, some other authors assigned this band to the combination of the streching and deformation vibration of —SiOH groups, see [30] and references therein.

3.2.2. NIR of Pt/SBA-15 samples

Upon introduction of the Pt into the SBA-15 and further treatments (heating), the dominant absorption bands exhibit some very interesting features. This is depicted in Figs. 5–7 for spectral regions 7600–6500, 6000–5000 and 5000–4200 cm^{-1}, respectively. The intensity of the first overtone band at 7326 cm^{-1} (Fig. 5) for Pt/SBA-15 samples indicates that the decrease of the silanol population is more prominent for Pt/SBA-15, DP, however, a significant decrease in the silanol number was also obtained for the Pt/SBA-15, WI sample. Both samples were found to exhibit a decrease in intensity of the bands assigned to silanols interacting with water (7141 and 6856 cm^{-1}). Similarly, the band arising from the interparticle contact at 7425 cm^{-1} is also less intense for both platinum containing samples. The second region of the spectral profile at around 5270 cm^{-1}, depicted in Fig. 6, reveals that both impregnated samples contain a slightly higher amount of water, arising from the aqueous environment used in the process. The water content also influences the intensity of the prominent silanol band at 7326 cm^{-1} as observed for the Pt containing materials

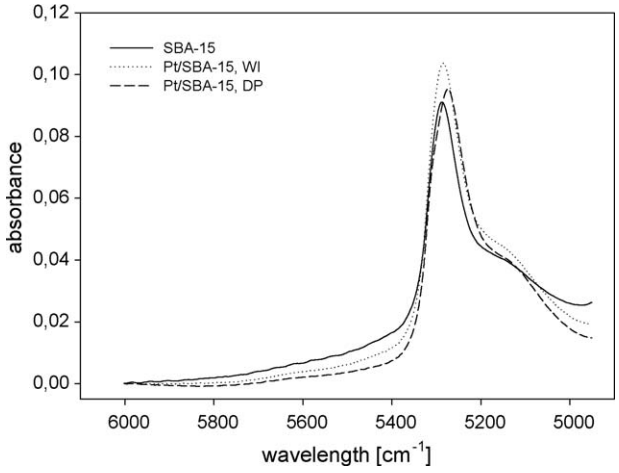

Fig. 6. Reflectance NIR spectra (6000–5000 cm^{-1}) of the parent SBA-15 and SBA-15 functionalized with Pt via DP and WI methods.

(Fig. 5) [26]. The splitting of the 4526 cm^{-1} band for the Pt/SBA-15, DP into three components is observed (Fig. 7). This has been also observed by other authors when a sol–gel glass heated to 1000 °C was exposed to ambient conditions. Subsequently, the band at 4555 cm^{-1} was attributed to the isolated SiOH groups, while the two others centered at 4518 and 4460 cm^{-1} were attributed to SiOH groups hydrogen bonded to water molecules [26].

3.2.3. NIR of SBA-15 upon the DP and WI treatment

In order to correctly interpret the loss of silanol groups observed for Pt containing samples and monitored as the decrease of intensity of the prominent silanols band at 7326 cm^{-1}, it is useful to resolve the impact of each pathway on the silanol population. Therefore, blank experiments were performed where SBA-15 was exposed to the same procedure as used in the DP and WI methods, but without the use of the platinum precursor.

Spectra obtained in the region 7600–6500 cm^{-1} for the WI *treated* and DP *treated* samples are shown in Figs. 8 and 9 respectively. Noticeable features of the prominent silanol band at about 7300 cm^{-1} are its shift towards a lower wavenumber and the broadening as compared to the Pt containing samples. This shift has previously been attributed to the structural changes of the siliceous materials, specifically, that not only the silica network has been consolidated but also the O–H silanol bond has been

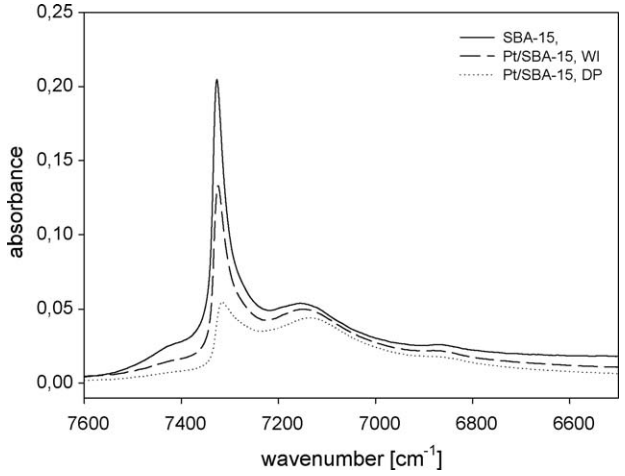

Fig. 5. Reflectance NIR spectra (7600–6500 cm^{-1}) of the parent SBA-15 and SBA-15 functionalized with Pt via DP and WI methods.

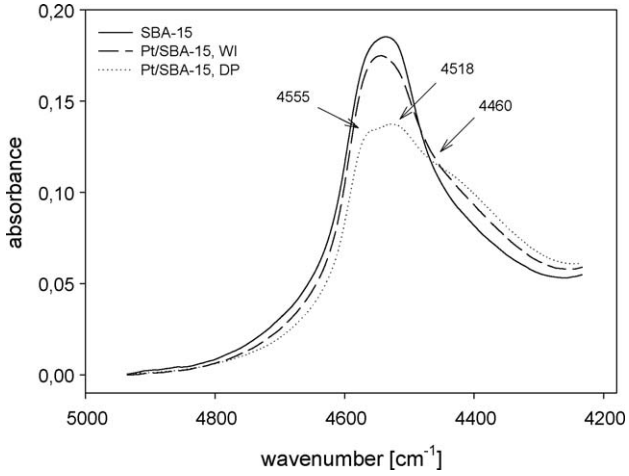

Fig. 7. Reflectance NIR spectra (4900–4300 cm^{-1}) of the parent SBA-15 and SBA-15 functionalized with Pt via DP and WI methods.

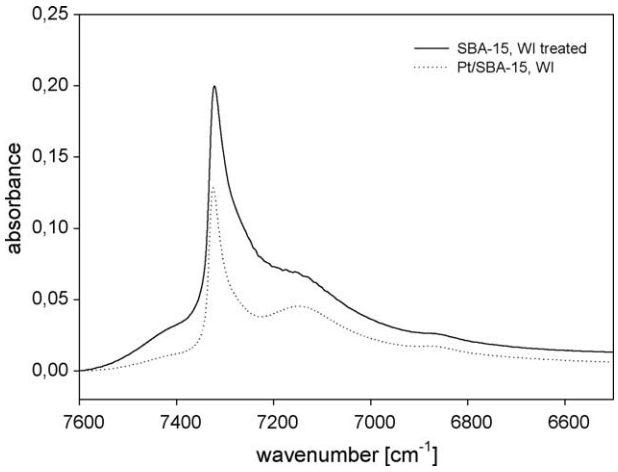

Fig. 8. Reflectance NIR spectra (7600–6500 cm^{-1}) of the Pt/SBA-15 prepared via WI method and SBA-15 exposed to an identical treatment as in the WI method (drying and mild calcination at 300 °C) but without use of the Pt precursor.

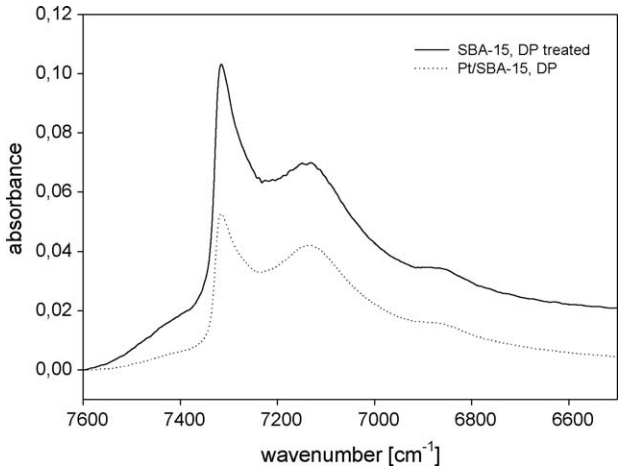

Fig. 9. Reflectance NIR spectra (7600–6500 cm^{-1}) of the Pt/SBA-15 prepared via DP method and SBA-15 exposed to an identical treatment as in the DP method (heating the parent SBA-15 at 90 °C in aqueous solution for approximately 20 h) but without use of the Pt precursor.

strengthened and/or shortened, while the broadening has been attributed to a change of the environment of the silanol groups from the surface to the interior of the silica network [26]. As a similar change is not seen on the functionalized samples, we propose that Pt retards changes occurring in the SBA-15 structure.

The WI *treated* sample exhibits only a mild reduction of the silanol groups as compared to the parent SBA-15, while the SBA-15, DP *treated* sample exhibits a significant decrease in the number of silanols. Possible reasons for such a behavior will be discussed in the NMR section. As indicated in Figs. 8 and 9, there is a difference in the silanol population between the treated, un-functionalized samples and samples containing Pt. We propose that the additional loss of silanols detected for the Pt containing SBA-15 may be due to the interaction with Pt. The importance of acidic oxygen-containing groups in the anchoring of the metal precursor onto a catalyst support has been shown by others for the homogenous deposition precipitation (HDP) of Pt onto carbon-nanofibers (CNF) [5]. Our study indicates that on the calcined solids, independently of the pathway, the metallic Pt may be anchored to the surface of SBA-15 through the silanols. Another hypothesis on the additional loss of silanols detected on the Pt containing samples could be an interaction of the ligands originating from the decomposition of the Pt precursors with the surface of silica. However, the NIR spectral profiles recorded on the Pt containing or treated samples did not show any bands corresponding to NH_x or Cl moieties, indicating that most of the ligands are removed during the calcination.

Another important consequence of the change of the silanols number observed on the treated, un-functionalized samples is the impact on the textural properties of the parent SBA-15. The impact of the slightly acidic impregnation (pH 3) without using a metal precursor on the textural changes of mesoporous SBA-15 structure was studied by others by means of N_2 adsorption–desorption and low angle XRD using synchrotron radiation [34]. It was found that such treatment leads to a slight decrease in BET surface area and pore volume, which was attributed to an additional calcination step. Here we measured surface area, pore volume and micropore volume on the DP *treated* sample, resulting in values of 350 m^2/g, 0.94 and 0.015 cm^3/g, respectively. All values are significantly lower as compared to the parent SBA-15, but on the other hand slightly above those obtained for the Pt/SBA-15, DP sample (Table 1). Therefore, the DP treatment itself is responsible for the textural properties of the Pt/SBA-15, DP sample, while the presence of Pt causes very modest changes in surface area, pore and micropore volume.

3.3. ^{29}Si MAS NMR characterization of SBA-15 and Pt/SBA-15

The fact that some structural changes occur on the Pt/SBA-15 samples has already been shown from the evaluation of XRD and N_2 sorption data and was also further suggested by the NIR data. Thus, it is of interest to explore the consequences of the changes in long-range order on the eventual corresponding changes in short-range order of SBA-15.

It was also pointed out above that the geminal silanol groups cannot be distinguished by means of NIR, due to the vibrational modes of these species which are expected to be very close to those of the isolated silanols [30]. On the other hand, the ^{29}Si MAS NMR spectrum of a siliceous material typically exhibits three Q^n bands assigned to ^{29}Si nuclei shielded by different binding environments. The low intensity Q^2 peak at −91 ppm is attributed to the geminal silanol groups $(\equiv SiO)_2Si(OH)_2$, the Q^3 at 101 ppm is assigned to the isolated silanols $(\equiv SiO)_3SiOH$, and the Q^4 band centered at −110 ppm is due to silicons of the $(\equiv SiO)_4Si$ type [35,36]. The latter band represents a silicon population in a fully condensed framework, while the Q^2 and Q^3 bands represent incompletely

Table 1
Physiochemical properties of ordered materials obtained from XRD and N2 adsorption–desorption.

Sample	d^a (nm)	Surface area (m^2/g)	Pore diameter (nm)	Wall thickness (nm)	Mesopore volume (cm^3/g)	Mesopore volume (cm^3/g)	Pt content (wt. %)
SBA-15	9.0	1070	5.8	3.5	1.18	1.18	–
Pt/SBA-15, WI	9.2	860	5.8	3.7	1.02	1.02	0.38
Pt/SBA-15, WI	9.2	330	8.3	1.3	0.87	0.87	0.25

[a] Interplanar spacing of primary reflection.

condensed silicon atoms. However, the monitoring of the silicons bearing –OH groups is usually performed by means of the ^{1}H ^{29}Si cross-polarisation method conducted under magic angle spinning conditions (CP/MAS NMR) at different contact times [22,31]. By use of the latter method, a strong enhancement of Q^2 and Q^3 bands is observed, which enables determination of the relative proportion of geminal and isolated silanols [22,31]. However, it has been pointed out that spectra obtained using the cross-polarization method do not show the whole siloxane population (Q^4) because the proton is too far from these silicon sites [35,37]. This indicates that ^{29}Si CP/MAS NMR may not be used when the purpose of the study is to explore the nature of the silica walls. Therefore, the bulk ^{29}Si MAS NMR measurement has been used in this study.

The NMR spectra of the examined materials are depicted in Fig. 10. The spectrum of the parent SBA-15 is well in agreement with existing literature, showing broad Q^n bands that are overlapping. This closely resembles reported NMR spectra of amorphous silicas [38] and the spectrum of mesoporous silica MCM-41 [39], suggesting a broad range of Si–O–Si (T–O–T) bond angles in this material. This is consistent with a framework that lacks precise repeats of Si positions at the second nearest neighbour (T–T) scale [39]. However, the Q^n bands are more distinguishable for the Pt containing materials, especially prominent for the sample prepared by the DP method, as the Q^n bands are detected at their regular positions for this material. These results strongly indicate that the functionalized materials, especially the Pt/SBA-15, DP sample, exhibit a better short-range order of the silica framework. We propose that this is related to a decrease in the silanol population as indicated by NIR. The WI *treated* sample exhibits a modest reduction of the silanol groups. This is most likely due to silanol consumption through dehydroxylation as proposed in the following equation:

$$\mathrm{SiOH} + \mathrm{OHSi} \rightarrow \mathrm{SiOSi} + \mathrm{H_2O} \quad (1)$$

The mild decrease in silanol population for the WI *treated* sample is not surprising as it has been shown that a significant reduction in the number of silanol groups due to dehydroxylation can only be expected for siliceous materials treated at temperatures higher (above 700 °C *in vacuo*) than those used in this study [27]. However, a slight decrease of the 7326 cm^{-1} band was observed already at 200 °C [27], which is also confirmed by our experiment. Furthermore, as already mentioned, the shift of the prominent silanol NIR band to 7320 cm^{-1} was observed, indicating the consolidation of the silica network. Based on this we propose that the improvement in the short-range order observed by means of ^{29}Si MAS NMR for the Pt/SBA-15, WI sample is associated with dehydroxylation of the framework caused by the additional calcination.

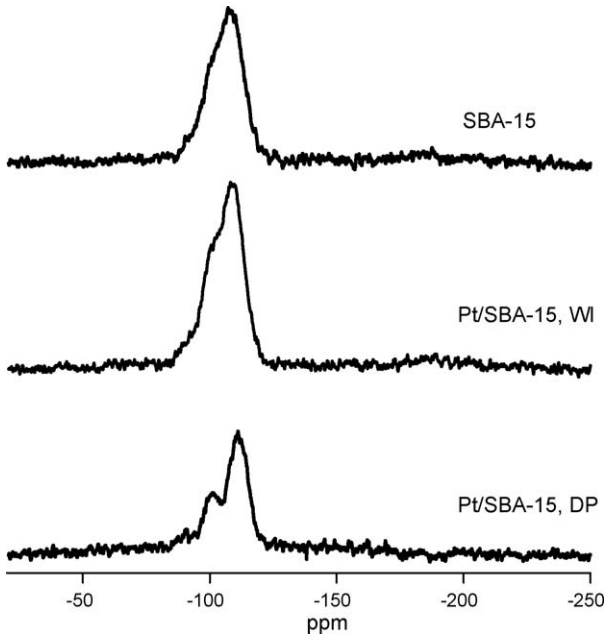

Fig. 10. ^{29}Si MAS NMR spectra of Pt/SBA-15 and SBA-15.

A significant improvement in the short-range periodicity as compared to parent SBA-15 is observed for the Pt/SBA-15, DP sample. Also in this case we propose that this is related to a decrease in the number of silanols as indicated by use of NIR.

When SBA-15 is exposed to an aqueous media it can dissolve due to hydrolysis of the Si–O–Si bond. It has been established that the solubility of silica and the dissolution rate depends on particle size, surface area, hydration state, impurities in silica, temperature and pH of the solution [33]. Here, the DP experiments were performed in the pH range 3–6.5, where, as it has been shown, the dissolution rate of silica is rather low [33,40]. However, it has also been pointed out that the rate increases proportionally with the surface area of the silica [33,40]. It should also be noted that the dissolution rate increases with increasing temperature [33]. According to the proposed mechanisms of silica dissolution [11,33] and the suggested kinetic model [40] available for this process it is likely that during the dissolution of the silica new silanol groups are generated on the surface. In parallel with the generation of the new silanol groups on the surface, $Si(OH)_4$ units are released as a product of silica dissolution. These units can condense, be ionized $[SiO(OH)_3]^-$ and form different types of monomeric, oligomeric, and polymeric chains, all negatively charged [11]. All these species are involved in the equilibrium of SBA-15 dissolution. Furthermore, the process is yet more complex as the $Si(OH)_4$ units can precipitate on the surface of SBA-15. This has been explained on the basis that silicon increases its coordination number from four to five as proposed for the case when $Si(OH)_4$ interacts with the surface [33].

If we want to implement these findings on SBA-15, it has to be reemphasised that the walls of SBA-15 exhibit a microporous region of *lower density* around the cylindrical aggregates [41]. The lower density region was suggested to be due to partial occlusion of the PEO copolymer chains in the silica matrix [41]. We assume that during the dissolution, occurring more progressively in the lower pH range of the DP experiment, the lower density region is involved. Subsequently, in the higher pH range of the DP experiment, the released $Si(OH)_4$ units precipitate on the surface of SBA-15. Upon the drying and calcination, this precipitated part of SBA-15 becomes more consolidated, which is accompanied by a significant decrease in the micropore volume. This process is suggested to be responsible for the improved short-range order of the Pt/SBA-15, DP sample as observed by means of ^{29}Si MAS NMR. However, in the light of the results obtained from the N_2 sorption it seems plausible that the process of the re-precipitation occurs in two ways. One way is the precipitation of the $Si(OH)_4$ units onto the remaining ordered mesoporous matrix while the rest of the siliceous species released during the dissolution condenses and agglomerates within the bulk solution. The latter process results in formation of non-ordered amorphous silica as detected by N_2 sorption.

4. Summary and conclusions

In this paper we have used several characterization techniques in order to bring more insight into some consequences of the

deposition–precipitation method when used to functionalize the mesoporous silica SBA-15 with Pt. Pt/SBA-15 prepared by a conventional wet impregnation method and parent SBA-15 were used as reference materials.

The N_2 sorption shows that the hydrothermal treatment involved in the DP method (heating the material at 90 °C for 20 h in aqueous solution) has a detrimental effect on the SBA-15 texture so that the final functionalized material contains larger fractions of non-ordered amorphous silica. On the other hand, the Pt containing sample prepared by the DP method posseses a better short-range order of the SBA-15 framework as shown by ^{29}Si MAS NMR.

It is suggested from the NIR spectroscopy data that the interaction between the mesoporous silica and Pt on calcined solid may be provided by silanol groups, through which the metallic Pt might be anchored to the surface of SBA-15.

Acknowledgments

The Norwegian Research Council is gratefully acknowledged for financial support through the Strategic University Programme *Scientific Design and Preparation of New Catalysts and Supports*, contract no. 153967/420. Aud M. Bouzga is acknowledged for recording the NMR data, and we thank Prof. M. Stöcker for his valuable comments on the manuscript.

References

[1] D. Zhao, J. Feng, Q. Huo, N. Melosh, G.H. Frederickson, B.F. Chmelka, G.D. Stucky, Science 279 (1998) 548.
[2] A. Taguchi, F. Schueth, Micropor. Mesopor. Mater. 77 (2004) 1.
[3] W. Yan, B. Chen, S.M. Mahurin, E.W. Hagaman, S. Dai, S.H. Overbury, J. Phys. Chem. B 108 (2004) 2793.
[4] C. Qi, M. Okumura, T. Akita, M. Haruta, Appl. Catal. A: Gen. 263 (2004) 19.
[5] M.L. Toebes, M.K. van der Lee, L.M. Tang, M.H. Huis in't Veld, J.H. Bitter, A.J. van Dillen, K.P. de Jong, J. Phys. Chem. B 108 (2004) 11611.
[6] J. Geus, A.J. Van Dillen, Preparation of supported catalysts by deposition precipitation, in: G. Ertl, H. Knoezinger, J. Weitkamp (Eds.), Preparation of Solid Catalysts, Wiley–VCH, Weinheim, 1999, pp. 460–487.
[7] H. Zhu, Z. Pan, B. Chen, B. Lee, S.M. Mahurin, S.H. Overbury, S. Dai, J. Phys. Chem. B 108 (2004) 20038.
[8] P. Burattin, M. Che, C. Louis, J. Phys. Chem. B 103 (1999) 6171.
[9] W. Yan, V. Petkov, S.M. Mahurin, S.H. Overbury, S. Dai, Catal. Commun. 6 (2005) 404.
[10] M.K. van der Lee, A.J. Van Dillen, J.H. Bitter, K.P. de Jong, J. Am. Chem. Soc. 127 (2005) 13573.
[11] P. Burattin, M. Che, C. Louis, J.Phys. Chem. B 102 (1998) 2722.
[12] F.-S. Xiao, Top. Catal. 35 (2005) 9.
[13] F. Zhang, Y. Yan, H. Yang, Y. Meng, C. Yu, B. Tu, D. Zhao, J. Phys. Chem. B 109 (2005) 8723.
[14] S. Chytil, W.R. Glomm, I. Kvande, Z. Tiejun, J.C. Walmsley, E.A. Blekkan, Top. Catal. 45 (2007) 93.
[15] J.C.P. Broekhoff, J.H. De Boer, J. Catal. 10 (1968) 377.
[16] M. Hartmann, A. Vinu, Langmuir 18 (2002) 8010.
[17] S. Chytil, W.R. Glomm, E. Vollebekk, H. Bergem, J. Walmsley, J. Sjoeblom, E.A. Blekkan, Micropor. Mesopor. Mater. 86 (2005) 198.
[18] J. Zhu, Z. Konya, V.F. Puntes, I. Kiricsi, C.X. Miao, J.W. Ager, A.P. Alivisatos, G.A. Somorjai, Langmuir 19 (2003) 4396.
[19] S. Chytil, W.R. Glomm, I. Kvande, Z. Tiejun, E.A. Blekkan, Stud. Surf. Sci. Catal. 162 (2006) 513.
[20] J. Perez-Ramirez, J.M. Garcia-Cortes, F. Kapteijn, G. Mul, J.A. Moulijn, C. Salinas-Martinez de Lecea, Appl. Catal. B: Environ. 29 (2001) 285.
[21] R.M. Rioux, H. Song, J.D. Hoefelmeyer, P. Yang, G.A. Somorjai, J. Phys. Chem. B 109 (2005) 2192.
[22] G. Engelhardt, Trends Analyt. Chem. 8 (1989) 343.
[23] G. Engelhardt, D. Michel, High-Resolution Solid-State NMR of Silicates and Zeolites, John Wiley & Sons, New York, 1987.
[24] X. Gao, I.E. Wachs, J. Catal. 192 (2000) 18.
[25] J.H. Anderson, K.A. Wickersheim, Surface Sci. 2 (1964) 252.
[26] C.C. Perry, X. Li, J. Chem. Soc., Faraday Trans. 87 (1991) 3857.
[27] C.C. Perry, X. Li, J. Chem. Soc., Faraday Trans. 87 (1991) 761.
[28] C.C. Harrison, X. Li, I. Hopkinson, S.E. Stratford, A.G. Orpen, J. Chem. Soc., Faraday Trans. 89 (1993) 4115.
[29] T. Vralstad, W.R. Glomm, M. Ronning, H. Dathe, A. Jentys, J.A. Lercher, G. Oye, M. Stocker, J. Sjoblom, J. Phys. Chem. B 110 (2006) 5386.
[30] B.A. Morrow, A.J. McFarlan, J. Phys. Chem. 96 (1992) 1395.
[31] I.G. Shenderovich, G. Buntkowsky, A. Schreiber, E. Gedat, S. Sharif, J. Albrecht, N.S. Golubev, G.H. Findenegg, H.-H. Limbach, J. Phys. Chem. B 107 (2003) 11924.
[32] R.H. Doremus, J. Phys. Chem. 75 (1971) 3147.
[33] R.K. Iler, The Chemistry of Silica, John Wiley & Sons, Inc., New York, 1979.
[34] A.Y. Khodakov, V.L. Zholobenko, R. Bechara, D. Durand, Micropor. Mesopor. Mater. 79 (2005) 29.
[35] B. Humbert, J. Non-Cryst. Solids 191 (1995) 29.
[36] D.W. Sindorf, G.E. Maciel, J. Am. Chem. Soc. 105 (1983) 1487.
[37] S. Leonardelli, L. Facchini, C. Fretigny, P. Tougne, A.P. Legrand, J. Am. Chem. Soc. 114 (1992) 6412.
[38] G.E. Maciel, D.W. Sindorf, J. Am. Chem. Soc. 102 (1980) 7606.
[39] J.S. Beck, J.C. Vartuli, W.J. Roth, M.E. Leonowicz, C.T. Kresge, K.D. Schmitt, C.T.W. Chu, D.H. Olson, E.W. Sheppard, J. Am. Chem. Soc. 114 (1992) 10834.
[40] W. Vogelsberger, A. Seidel, G. Rudakoff, J. Chem. Soc., Faraday Trans. 88 (1992) 473.
[41] M. Imperor-Clerc, P. Davidson, A. Davidson, J. Am. Chem. Soc. 122 (2000) 11925.